PROCEEDINGS OF SCIENCE

Solar neutrinos from the CNO fusion cycle: Borexino discovery and implications for the solar physics

Livia Ludhova[a,b,*] **on behalf of the Borexino Collaboration**

[a] *Forschungszentrum Jülich, Institut für Kernphysik, 52425 Jülich, Germany*

[b] *RWTH Aachen University, III. Physikalisches Institut B 52062 Aachen, Germany*

E-mail: l.ludhova@fz-juelich.de

Our Sun is powered by the fusion of hydrogen into helium that proceeds in the solar core via two distinct mechanisms: dominant proton-proton (*pp*) chain and sub-dominant Carbon-Nitrogen-Oxygen (CNO) cycle. Solar neutrinos are emitted in electron-flavour eigenstate along several distinct reactions of both cycles, each characterized by a specific energy spectrum and flux. These so-called solar neutrinos are the only direct probe of the energy production mechanism in the Sun and stars in general. Borexino, a 280-ton liquid scintillator detector that was taking data from May 2007 to October 2021 at the Laboratori Nazionali del Gran Sasso (LNGS) in Italy, is the only experiment to perform a comprehensive spectroscopy of *pp* chain solar neutrinos and to prove the existence of CNO cycle. This was made possible thanks to an unprecedented radio-purity and thermal stability of the detector. This contribution is focused on the Borexino measurement of CNO solar neutrinos, that allowed us to exclude the absence of CNO signal with high statistical significance. In addition, we used the CNO flux measurement together with the ^{8}B flux stemming from the global analysis of all solar neutrino data to evaluate the abundance of C and N with respect to H in the Sun with solar neutrinos for the first time. Our result agrees with the high metallicity spectroscopic photospheric measurements and shows a $\sim 2\sigma$ tension with the low metallicity ones.

38th International Cosmic Ray Conference (ICRC2023)
26 July - 3 August, 2023
Nagoya, Japan

[*] Speaker

PoS(ICRC2023)970

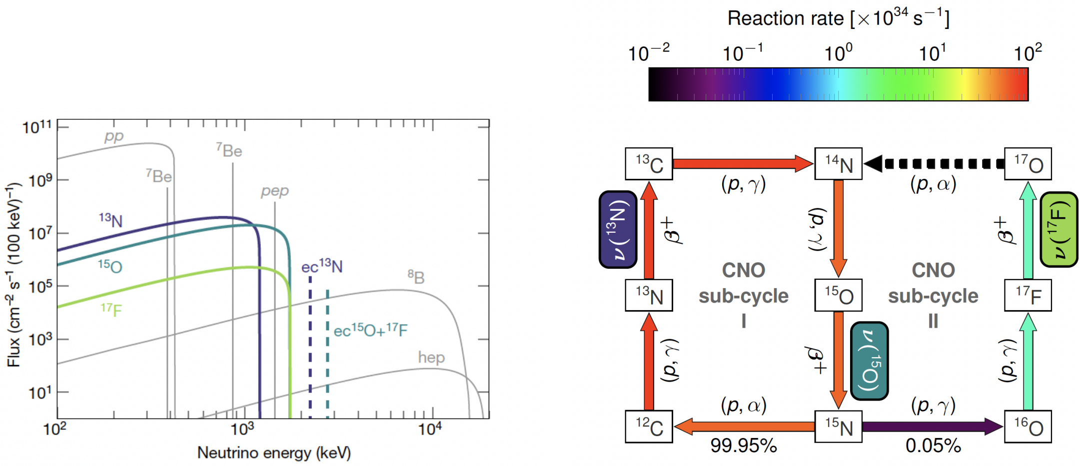

(a) (b)

Figure 1: (a) Energy spectra of solar neutrinos from the *pp* chain (grey; representing *pp*, *pep*, ^{7}Be, ^{8}B and *hep* neutrinos) and from the CNO cycle (in colour). (b) The double CNO cycle in the Sun, in which sub-cycle I is dominant. The coloured arrows indicate the reaction rates integrated over the volume of the Sun.

1. Introduction

Our Sun is powered by two distinct series of nuclear reactions occurring in the hot solar core, in which hydrogen is fused to helium. The *pp* chain provides about 99% of solar energy. In the sub-dominant CNO cycle this fusion is catalyzed by the presence of carbon, nitrogen, and oxygen. The relative rates of these processes depend on the temperature. For the stars ~1.3 times heavier than the Sun, the CNO cycle dominates and thus represents principal mechanism of the stellar helium creation in the Universe. Solar neutrinos (νs) are emitted in both processes, being their only direct probe and prove of existence. The energy spectra of solar νs are shown in Fig. 1(a), where the fluxes are normalized according to the prediction of the Standard Solar Model (SSM) [1].

Several ν types are emitted in the *pp* chain, named after the interaction of origin: *pp* νs with the lowest energy spectrum and highest flux, mono-energetic ^{7}Be and *pep* νs, ^{8}B νs, and the only unobserved *hep* νs. The relatively low ^{8}B ν flux extends above 10 MeV and it is the only one accessible to the water-based Cherenkov detectors [2, 3] having a few-MeV energy threshold. Borexino, a liquid scintillator detector, is the only experiment that succeeded in real-time measurement of solar νs with such a low energy threshold to perform a comprehensive spectroscopy of *pp* chain [4] and to discover the CNO solar νs [5, 6].

The CNO cycle consists of two sub-cycles (Fig. 1(b)), called CN and NO: at the relatively low temperature of the solar core, sub-cycle CN is largely dominant at ~99% level and produces νs from the β-decays of ^{15}O and ^{13}N. The fusion catalyzed by C, N, and O provides direct information on the metallicity of the Sun's core, i.e., its abundance of elements heavier than helium.

Metallicity is a key input of the SSMs and is determined experimentally by the spectral analysis of the photosphere, sometimes complemented by studies of meteorites: while measurements from the past two decades (AGSS09met [7, 8], C11 [9], AAG21 [10]) have been suggesting a lower content of heavy elements with respect to the earlier ones (GS98 [11]), the most recent MB22 [12]

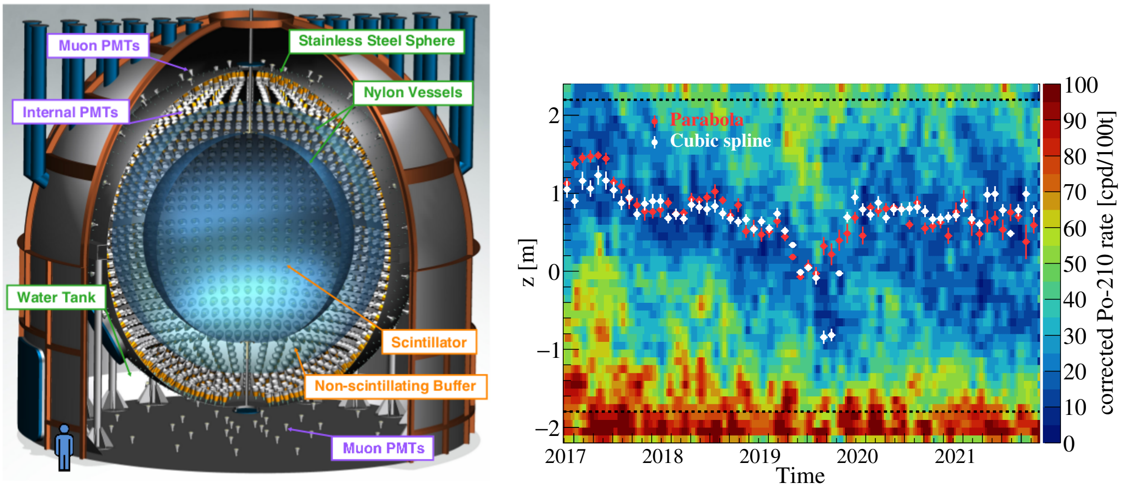

(a) (b)

Figure 2: (a) Scheme of the Borexino detector. (b) Time evolution of the ^{210}Po rate in the detector, visualized in terms of cylindrical z-slices of 0.1 m height and radius $\rho^2 = (x^2 + y^2) < 2\,\mathrm{m}^2$. The horizontal black dashed lines represent the z-cut used in the CNO analysis. The Low Polonium Field centers obtained from the monthly paraboloid fits with (white) and without (red) a cubic spline along the z-axis are also shown.

results point to a higher value. Noticeably, SSMs implementing the class of "low-metallicity" compositions fail to reproduce helioseismological measurements, while "high-metallicity" ones are in a better agreement with them [1, 12].

Metallicity impacts the SSM predictions of ^{8}B, ^{7}Be, and CNO ν fluxes significantly, but in an indirect way. The metal content affects the solar opacity, which in turn impacts the Sun's temperature profile, which ultimately controls the rate of nuclear reactions and ν emission. Thus, deriving information on metallicity from the measurements of solar νs presents a certain degree of ambiguity. However, in this respect, the CN cycle which is catalyzed by the C and N, is special: its flux has an additional, almost linear dependence on the abundances of these metals in the solar core, providing a unique handle for their non-ambiguous determination.

2. Borexino detector

Borexino was a large volume liquid scintillator experiment, located at Laboratori Nazionali del Gran Sasso in Italy, that took data from May 2007 until October 2021. The core of the detector [13] consisted of ~280 tonnes of liquid scintillator contained in a 4.25 m radius, 125 μm-thick nylon vessel. The concentric detector geometry, depicted in Fig. 2(a), was designed to shield the innermost scintillator from the radioactivity originating from external materials. The scintillation light was detected by nominally 2212 photomultiplier tubes (PMTs) mounted on a 7-m radius stainless steel sphere (SSS). Since the solar ν signal is rare and indistinguishable from natural radioactivity, radiopurity and background control, developed over more than 10 years for this purpose [14, 15], were the critical components in the success of the experiment. The underground location reduces the cosmic muon flux by a factor of $\approx 10^6$, while a water Cherenkov veto surrounding the SSS tags residual muons [16]. During the initial filling, the scintillator was purified to unprecedented levels of radiopurity [17], further improved [4] by operations performed in 2010-2011. Between 2015 - 2019, the Borexino detector was thermally stabilized to suppress the seasonal convection currents inside the scintillator volume [5].

3. CNO neutrinos: an experimental challenge

In Borexino, solar νs are detected via their elastic scattering off electrons, which induce signals characterized by continuous energy distributions even for mono-energetic νs, such as ^{7}Be or *pep*. For CNO νs, with energy extending up to 1740 keV, the electron spectrum is rather featureless with an end-point at 1517 keV and with an expected interaction rate of just a few counts per day (cpd) in 100 tonnes of scintillator. In addition, the CNO spectral shape is highly correlated with that of *pep* solar νs as well as with the β^- spectrum of ^{210}Bi, originating from the ^{210}Pb contamination of liquid scintillator. ^{210}Pb is not a dangerous background by itself, but due to its long-lifetime it is constantly producing ^{210}Bi. Note that in Borexino, the ^{210}Pb is out of equilibrium with the ^{238}U chain, which abundance in the scintillator was found negligible for solar ν analysis. The *pep* solar ν rate can be constrained with 1.4% precision, using the solar luminosity constraint and the global fit of independent solar ν data [18]. In order to extract the CNO solar ν signal, constraining the decay rate of ^{210}Bi is also necessary [18]. This can be achieved by measuring the α decay rate of the ^{210}Bi daughter, ^{210}Po, exploiting α/β particle discrimination techniques [19].

This procedure was severely limited by out-of-equilibrium ^{210}Po in the analysis volume, originating from the vessel surface and carried over by temperature-driven seasonal convective currents. The thermal stabilisation of the Borexino detector mentioned above was carried out to suppress this effect. This made possible the first evidence of CNO νs [5] using data collected from July 2016 until February 2020. An improved CNO measurement from 2022 [6] is based on data taken when the radiopurity and thermal stability of the detector was maximal, *i.e.*, between January 2017 and October 2021 (final Phase-III). The last part of the dataset features an unprecedented thermal stability and an enlarged volume of strongly reduced ^{210}Po contamination (see Fig. 2(b)), and therefore provides an improved ^{210}Bi constraint. Furthermore, the second half of 2016 was excluded, as it was still affected by an evident amount of out-of-equilibrium ^{210}Po. The overall exposure of the latest Borexino CNO spectral analysis is 1431.6 days $\times$ 71.3 tonnes.

4. Improved CNO measurement

To disentangle the CNO ν signal from other solar νs and backgrounds, we perform a multivariate fit simultaneously on two energy spectra between 320 keV and 2640 keV and on the radial distribution of selected events. The two energy spectra are obtained by dividing the selected events into two complementary datasets, depleted and enriched of cosmogenic ^{11}C using the *Three-Fold Coincidence* procedure [20]. The largest sensitivity to CNO νs comes from the ^{11}C-depleted spectrum [18] shown in Fig. 3(a), in which the CNO end-point is “unveiled" by the removal of about 90% of ^{11}C with >60% of the original exposure. All events must be reconstructed in a centrally located fiducial volume with a mass of $71.3^{+0.5}_{-1.3}$ tonnes. The shapes of all signal and background components are obtained with a full Geant4-based Monte Carlo simulation [21] with an improved

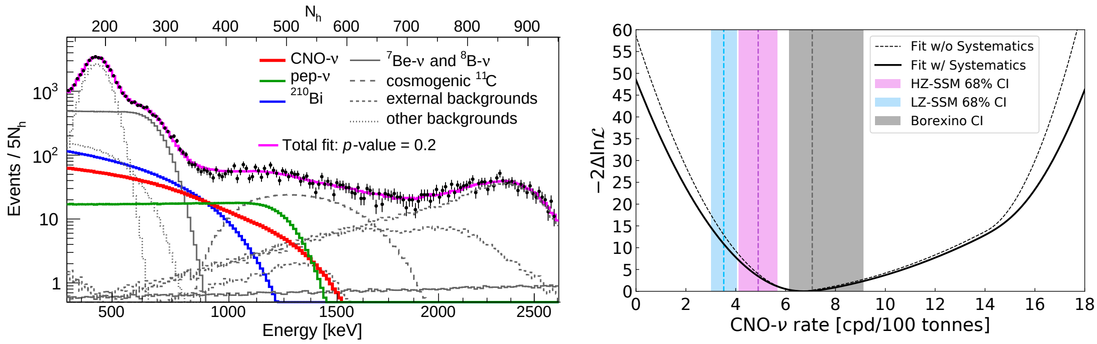

(a) (b)

Figure 3: (a) Spectral fit (magenta) of the Borexino Phase-III data (black points) from January 2017 to October 2021 with a suppressed cosmogenic ^{11}C background (grey dashed). CNO νs are shown in red. The rates of *pep* νs (green) and ^{210}Bi (blue) were constrained in the fit based on independent data. The energy estimator N_{h}, in which the fit is performed, represents the number of detected photoelectrons, normalized to 2,000 PMTs. (b) CNO ν rate negative log-likelihood ($-2\Delta\ln\mathcal{L}$) profile obtained from the spectral fit (dashed black line) and after folding in the systematic uncertainties (black solid line). The blue, violet, and grey vertical bands show 68% confidence intervals (CI) for the low metallicity SSM B16-AGSS09met ((3.52 ± 0.52) cpd/100 tonnes) and the high metallicity SSM B16-GS98 ((4.92 ± 0.78) cpd/100 tonnes) predictions [1, 18], and the new Borexino result [6] including systematic uncertainty, respectively.

treatment of the time evolution of PMT's effective quantum efficiencies based on the low-energy ^{14}C data. We note that Borexino is sensitive neither to the small dependence of the shape of solar ν components on the oscillation parameters, nor on the relative ratio of the individual CNO components. Thus, in the Monte Carlo production we assume the standard 3-flavour ν oscillations and the ^{13}N, ^{15}O, and ^{17}F relative contributions to the CNO flux according to SSM B16-GS98 [1].

A constraint on ^{210}Bi is evaluated from the minimum rate of its daughter ^{210}Po in the volume of *Low Polonium Field* (LPoF), which is quantified via a fit with a 2D paraboloid equation as in [5]. Since we cannot exclude small levels of out-of-equilibrium ^{210}Po from residual scintillator convection, we consider this an upper limit on ^{210}Bi. The z position of the LPoF was slightly changing in time due to residual convective motions as it is shown in Fig. 2(b). From August 2020, the LPoF size has significantly increased and its position was stabilized. The ^{210}Bi upper limit of (10.8 ± 1.0) cpd/100 tonnes including all systematic uncertainties was obtained via a fit of time-aligned LPoF. The major systematic contribution of 0.68 cpd/100 tonnes is associated with the ^{210}Bi spatial uniformity in the fiducial volume, a required condition to apply the ^{210}Bi constraint in a volume ~3 times larger than the LPoF. In the final fit with constrained ^{210}Bi and *pep*, the rates of additional backgrounds, i.e., the external γs from ^{40}K, ^{208}Tl, and ^{214}Bi, ^{85}Kr and ^{210}Po in the scintillator, cosmogenic ^{11}C, and ^{7}Be solar νs are free fit parameters. We obtain the CNO ν interaction rate with zero threshold of $6.6^{+2.0}_{-0.7}$ cpd/100 tonnes. The corresponding negative log-likelihood profile (dashed line in Fig. 3(b)) is asymmetric since the upper limit on ^{210}Bi impacts only the left part of the CNO profile. The right part of the CNO profile is unconstrained by the penalty and exploits the small difference between the CNO and ^{210}Bi spectral shapes. The total systematic uncertainty of $^{+0.5}_{-0.4}$ cpd/100 tonnes was evaluated with the same toy-Monte-Carlo-based method as in [5]. The final result on the CNO ν interaction rate with zero-threshold is $6.7^{+2.0}_{-0.8}$ cpd/100 tonnes. This result

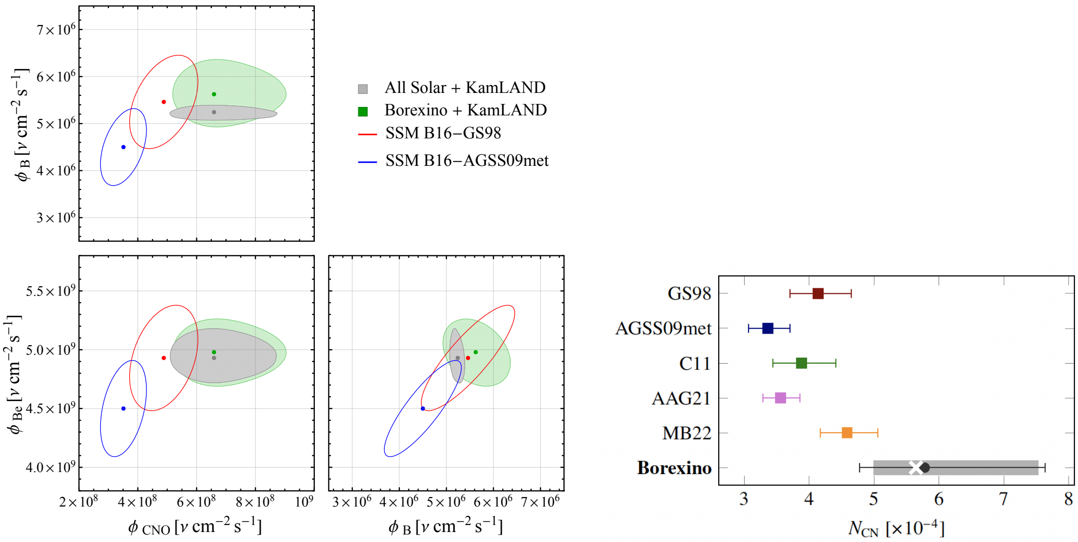

(a) (b)

Figure 4: (a) Global analysis results: 1σ regions allowed by all solar (Borexino only) νs and KamLAND reactor ν data shown in grey (green) in the Φ_B-Φ_{Be}, Φ_B-Φ_{CNO}, and Φ_{Be}-Φ_{CNO} planes. The 1σ predictions [1] of high-metallicity SSM B16-GS98 (red) and low-metallicity SSM B16-AGSS09met (blue) are also shown. (b) Comparison of abundance of $(C+N)/H$ in the solar photosphere, N_{CN}, from the spectroscopy of solar photosphere (squares) and from the Borexino CNO ν measurement (circle). The gray area highlights the uncertainty due to the precision of the CNO ν rate measurement. The white cross marks the result of the very same study repeated changing the reference SSM from the B16-GS98 to the B16-AGSS09met.

excludes the no-CNO-signal hypothesis at about 7σ C.L. Using the density of electrons in the scintillator of $(3.307 \pm 0.015) \times 10^{31}\ e^-/100$ tonnes, and assuming Mikheyev-Smirnov-Wolfenstein flavour conversion in matter [22–24] and the ν oscillation parameters from [25], the measured rate with systematic uncertainty is converted into a CNO solar ν flux on Earth of $6.6^{+2.0}_{-0.9} \times 10^8\ \mathrm{cm^{-2}\,s^{-1}}$.

5. Implications for solar physics

We perform a global analysis of all solar ν data to test their compatibility with the SSM B16 predictions on solar ν fluxes [1]. We follow the procedure discussed in [4, 17] and include, with the new CNO ν rate measurement [6], the data from radiochemical experiments [28–30], ^{8}B-ν data from SNO [2, 31] and Super-Kamiokande [3, 32], and Borexino Phase II [4] results on ^{7}Be and ^{8}B νs, as well as the KamLAND reactor $\bar{\nu}_e$ data [33] to better constrain Δm^2_{21}. The fluxes Φ of ^{8}B, ^{7}Be, and CNO neuttrinos, as well as Δm^2_{12} and θ_{12} are left free in the fit, while θ_{13}, having a negligible impact on the analysis, was fixed according to [25]. The results are shown in Fig. 4(a). We find that the p-value of the comparison between the low-metallicity SSM B16-AGSS09met predictions and the global analysis results worsens from 0.327 to 0.028 when including the CNO measurement. The same happens in the comparison with Borexino-only data, where the p-value lowers from 0.196 to 0.018 when including CNO. On the other hand, the high-metallicity SSM B16-GS98 is fully compatible with both the global analysis and the Borexino-only results in all cases (p-value = 0.462 and 0.554 including CNO, respectively). Following the procedure described in [4], a frequentist hypothesis test using only Borexino CNO, ^{7}Be, and ^{8}B ν fluxes, disfavors the SSM B16-AGSS09met at 3.1σ C.L. (p-value = $9.1 \cdot 10^{-4}$) as an alternative to SSM B16-GS98.

The interpretation of the observed tension between data and SSM B16-AGSS09met predictions is not straightforward due to the degeneracy between metallicity, opacity, and other inputs to the SSM. More information on metallicity can be gathered by exploiting the direct dependence of the CNO cycle on the C and N abundances in the core of the Sun, in combination with the precise measurement of the ^{8}B-ν flux, as suggested in [34, 35] and discussed specifically for Borexino in [18]. The resulting C + N abundance with respect to the H in the photosphere is $N_{\rm CN} = (5.78^{+1.86}_{-1.00}) \times 10^{-4}$. This represents the first determination of the abundance of C + N in the Sun using νs. Our result is compared to spectroscopic measurements of the photosphere in Fig. 4(b). It is in good agreement with the recent MB22 [12] and the outdated GS98 [11] compilations, while it shows a moderate ~2σ tension with the values of AGSS09met [7, 8] and its recent update AAG21 [10].

6. Summary and outlook

Borexino presented a measurement of the CNO solar νs with an improved uncertainty of $^{+30\%}_{-12\%}$ on its rate [6]. This result reinforces the one previously published by Borexino in 2020 [5], now further increasing the detection significance against the null hypothesis to about 7σ C.L. We included this new result in the global analysis of all solar and KamLAND reactor ν data. We found the resulting solar ν fluxes to be in agreement with the “high metallicity" SSM B16-GS98 [1], while a moderate tension is observed when “low metallicity" AGSS09met is used for the SSM prediction. In addition, we used the CNO ν measurement together with the ^{8}B ν flux from the global analysis to determine the C + N abundance in the Sun, breaking the ambiguity due to the opacity/metallicity degeneracy. The C + N abundance determined with this method agrees very well with the so-called high-metallicity compilations (MB22 [12], GS98 [11]) and features a moderate ~2σ tension with the low-metallicity ones (AGSS09met [7, 8], C11 [9], AAG21 [10]). A more precise measurement of the CNO ν flux by future experiments [26] could definitively assess the long-standing metallicity controversy and constrain the range of possible non-standard solar models [8, 27].

References

[1] Vinyoles N. et al., *Astrop. Phys. J.* **835** (2017) 202.

[2] Aharmim B. et al. (SNO Collaboration), *Phys. Rev. C* **88** (2013) 025501.

[3] K. Abe et al. (Super-Kamiokande Collaboration), *Phys. Rev. D* **94** (2016) 052010.

[4] Agostini M. et al. (Borexino Collaboration), *Nature* **562** (2018) 496.

[5] Agostini M et al. (Borexino Collaboration), *Nature* **587** (2020) 577.

[6] Appel S. et al. (Borexino Collaboration), *Phys. Rev. Let.* **129** (2022) 252701.

[7] Asplund M. et al., *Annu. Rev. Astron. Astrophys.* **47** (2009) 481.

[8] Serenelli A. M., Haxton W., and Pena-Garay C., *Astrophys. J.* **743** (2011) 24.

[9] Caffau E. et al., *Sol. Phys.* **268** (2011) 255.

[10] Asplund M., Amarsi A. M., and Grevesse N., *Astron. Astrophys.* **653** (2021) A141.

[11] Grevesse N. and Sauval A., *Space Sci. Rev.* **85** (1998) 161.

[12] Magg E. et al., *Astron. Astrophys.* **661** (2022) A140.

[13] Alimonti G. et al. (Borexino Collaboration), *Astropart. Phys.* **16** (2002) 205.

[14] Benziger J. et al., *Nucl. Instrum. Methods Phys. Res. A* **587** (2008) 277.

[15] Alimonti G. et al. (Borexino Collaboration), *Nucl. Instrum. Meth. Phys. Res. A* **609** (2009) 58.

[16] Bellini G. et al. (Borexino Collaboration), *J. Instrum.* **6** (2011) P05005.

[17] Bellini G. et al. (Borexino Collaboration), *Phys. Rev. D* **89** (2014) 112007.

[18] Agostini M. (Borexino Collaboration), *Eur. Phys. J. C* **80** (2020) 1091.

[19] Villante F. et al., *Phys. Lett. B* **701** (2011) 336.

[20] Agostini M. et al. (Borexino Collaboration), *Eur. Phys. Journal C* **81** (2021) 1075.

[21] Agostini M. et al. (Borexino Collaboration), *Astrop. Phys.* **97** (2018) 136.

[22] Wolfenstein L., *Phys. Rev. D* **17** (1978) 2369.

[23] Mikheyev S. and Smirnov A. *Sov. J. Nucl. Phys.* **42** (1985) 913.

[24] de Holanda P., Liao W., and Smirnov A., *Nucl. Phys.* B **702** (2004) 307.

[25] Esteban I. et al., *J. High Energy Phys.* **09** (2020) 178.

[26] Abusleme A. et al. (JUNO Collaboration), arXiv:2303.03910 and accepted for publication in *J. Cosm. Astrop. Phys.*

[27] Zhang Q.-S., Li Y., and Christensen-Dalsgaard J., *Astrophys. J.* **881** (2019) 103.

[28] Cleveland B. T. et al., (Homestake Collaboration), *Astrophys. J.* **496** (1998) 505.

[29] Abdurashitov J. N. et al. (SAGE Collaboration), *Phys. Rev. C* **80** (2009) 015807.

[30] Kaether F. et al., *Phys. Lett. B* **685** (2010) 47.

[31] Aharmim B. et al. (SNO Collaboration), *Phys. Rev. Lett.* **101** (2008) 111301.

[32] Hosaka J. et al. (Super-Kamiokande Collaboration), *Phys. Rev. D* **73** (2006) 112001.

[33] Gando A. et al. (KamLAND Collaboration), *Phys. Rev. D* **83** (2011) 052002.

[34] Haxton W. C. and Serenelli A. M., *Astrophys. J.* **687** (2008) 678.

[35] Serenelli A., Peña-Garay C., and Haxton W. C., *Phys. Rev. D 87* (2013) 043001.

Full Authors List: Borexino Collaboration

L. Ludhova[1,2], S. Appel[3], Z. Bagdasarian[1,a], D. Basilico[4], G. Bellini[4], J. Benziger[5], R. Biondi[6], B. Caccianiga[4], F. Calaprice[7], A. Caminata[8], P. Cavalcante[9,b], A. Chepurnov[10], D. D'Angelo[4], A. Derbin[11], A. Di Giacinto[6], V. Di Marcello[6] X.F. Ding[7], c, A. Di Ludovico[7,b], L. Di Noto[8], I. Drachnev[11], D. Franco[12], C. Galbiati[7,13], C. Ghiano[6], M. Giammarchi[4], A. Goretti[7,b], A.S. Göttel[1,2], M. Gromov[10,14], D. Guffanti[15,d], Aldo Ianni[6], Andrea Ianni[7], A. Jany[16], V. Kobychev[17], G. Korga[18,19], S. Kumaran[1,2,e], M. Laubenstein[6], E. Litvinovich[20,21], P. Lombardi[4], I. Lomskaya[11], I. Machulin[20,21], J. Martyn [15], E. Meroni[4], L. Miramonti[4], M. Misiaszek[16], V. Muratova[11], R. Nugmanov[20], L. Oberauer[3], V. Orekhov[15], F. Ortica[22], M. Pallavicini[8], L. Papp[3], L. Pelicci[1,2], Ö. Penek[1], L. Pietrofaccia[7,b], N. Pilipenko[11], A. Pocar[22], G. Raikov[20], M.T. Ranalli[6], G. Ranucci[4], A. Razeto[6], A. Re[4], M. Redchuk[1,2,f], N. Rossi[6], S. Schönert[3], D. Semenov,[11], G. Settanta[1,g], M. Skorokhvatov[20,21], A. Singhal[1,2], O. Smirnov[14], A. Sotnikov[14], R. Tartaglia[6], G. Testera[8], E. Unzhakov[11], F. Villante[11], A. Vishneva[14], R.B. Vogelaar[9], F. von Feilitzsch[3], M. Wojcik[16], M. Wurm[15], S. Zavatarelli[8], K. Zuber[25], and G. Zuzel[16].

[1]Institut für Kernphysik, Forschungszentrum Jülich, 52425 Jülich, Germany. [2]III. Physikalisches Institut B, RWTH Aachen University, 52062 Aachen, Germany. [3]Physik-Department, Technische Universität München, 85748 Garching, Germany. [4]Dipartimento di Fisica, Università degli Studi e INFN, 20133 Milano, Italy. [5]Chemical Engineering Department, Princeton University, Princeton, NJ 08544, USA. [6]INFN Laboratori Nazionali del Gran Sasso, 67010 Assergi (AQ), Italy. [7]Physics Department, Princeton University, Princeton, NJ 08544, USA. [8]Dipartimento di Fisica, Università degli Studi e INFN, 16146 Genova, Italy. [9]Physics Department, Virginia Polytechnic Institute and State University, Blacksburg, VA 24061, USA. [10]Lomonosov Moscow State University Skobeltsyn Institute of Nuclear Physics, 119234 Moscow, Russia. [11]St. Petersburg Nuclear Physics Institute NRC Kurchatov Institute, 188350 Gatchina, Russia. [12]AstroParticule et Cosmologie, Université Paris Diderot, CNRS/IN2P3, CEA/IRFU, Observatoire de Paris, Sorbonne Paris Cité, 75205 Paris Cedex 13, France. [13]Gran Sasso Science Institute, 67100 L'Aquila, Italy. [14]Joint Institute for Nuclear Research, 141980 Dubna, Russia. [15]Institute of Physics and Excellence Cluster PRISMA+, Johannes Gutenberg-Universität Mainz, 55099 Mainz, Germany. [16]M. Smoluchowski Institute of Physics, Jagiellonian University, 30348 Krakow, Poland. [17]Kiev Institute for Nuclear Research, 03680 Kiev, Ukraine. [18]Department of Physics, Royal Holloway University of London, Egham, Surrey,TW20 0EX, UK. [19]Institute of Nuclear Research (Atomki), Debrecen, Hungary. [20]National Research Centre Kurchatov Institute, 123182 Moscow, Russia. [21]National Research Nuclear University MEPhI (Moscow Engineering Physics Institute), 115409 Moscow, Russia. [22]Dipartimento di Chimica, Biologia e Biotecnologie, Università degli Studi e INFN, 06123 Perugia, Italy. [23]
address[UMass]Amherst Center for Fundamental Interactions and Physics Department, University of Massachusetts, Amherst, MA 01003, USA. [24]ddress[Aquila]Dipartimento di Scienze Fisiche e Chimiche, Università dell'Aquila, 67100 L'Aquila, Italy [25]Department of Physics, Technische Universität Dresden, 01062 Dresden, Germany

[a]Present address: University of California, Berkeley, Department of Physics, CA 94720, Berkeley, USA. [b]Present address: INFN Laboratori Nazionali del Gran Sasso, 67010 Assergi (AQ), Italy. cPresent address: IHEP Institute of High Energy Physics, 100049 Beijing, China. [d]Present address: Dipartimento di Fisica, Universit‡ degli Studi e INFN Milano-Bicocca, 20126 Milano, Italy. [e]Present address: Department of Physics and Astronomy, University of California, Irvine, California, USA. [f]Present address: Dipartimento di Fisica e Astronomia dellíUniversit‡ di Padova and INFN Sezione di Padova, Padova, Italy. gPresent address: Istituto Superiore per la Protezione e la Ricerca Ambientale, 00144 Roma, Italy.